Gauge-Origin-Independent Coupled Cluster Singles and Doubles Calculation of Magnetic Circular Dichroism of Azabenzenes and Phosphabenzene Using London Orbitals[†]

Thomas Kjærgaard,* Branislav Jansík, and Poul Jørgensen

Lundbeck Foundation Center for Theoretical Chemistry, Department of Chemistry, Aarhus University, Langelandsgade 140, DK-8000 Århus C, Denmark

Sonia Coriani

Dipartimento di Scienze Chimiche, Università degli Studi di Trieste, Via Licio Giorgieri 1, I-34127 Trieste, Italy

Josef Michl

Department of Chemistry and Biochemistry, University of Colorado, Boulder, Colorado, 80309-0215

A computational study of the Faraday $\mathscr{B}$ term of magnetic circular dichroism at the coupled cluster singles and doubles level is presented for pyridine, pyrazine, pyrimidine, and phosphabenzene. Gauge-origin independence is obtained by expressing the $\mathscr{B}$ term as a total derivative of the one-photon dipole transition strength and using London orbitals. The high quality of the coupled cluster singles and doubles (CCSD) $\mathscr{B}$ terms makes these useful for the assignment of experimental spectra. Previous assignments of the experimental spectra based on the qualitative perimeter model are confirmed by the CCSD results for the three azines, while a reassignment is proposed for phosphabenzene. For non-overlapping bands, the $\mathscr{B}$ terms calculated at the equilibrium geometries are in good agreement with the experimental values. For overlapping bands, large deviations occur. Attributing a line width to the calculated equilibrium $\mathscr{B}$ terms leads to a large cancellation of positive and negative contributions. This cancellation may result in a large displacement of the band center maximum, leading to a large uncertainty in the assignments of "vertical experimental excitation energies" (pyridine). Bands may also completely vanish due to such cancellation (phosphabenzene). Explicit consideration of the cancellation yields simulated theoretical spectra that are in good agreement with experiment once the theoretical spectra are parallel displaced. A major contribution for this parallel displacement is the shift in the excitation energies due to correlation beyond CCSD, as seen when comparing vertical CCSD and CC3 equilibrium-geometry excitation energies.

I. Introduction

When a molecule is exposed to a magnetic field, the field introduces a difference in the absorption coefficients for left- and right-circularly polarized light.[1,2] This difference is measured in magnetic circular dichroism (MCD) and may be rationalized in terms of three magnetic rotatory strengths, known as the Faraday $\mathscr{A}$, $\mathscr{B}$, and $\mathscr{C}$ terms.[3] The $\mathscr{B}$ term contributes regardless of the degeneracies of the involved states. It can be either positive (a negative band in the MCD spectrum) or negative (a positive peak in the MCD spectrum), and therefore, it represents a valuable supplement to UV spectra when it comes to identifying excited states, especially states hidden in UV spectra by overlapping bands.

A reliable theoretical determination of MCD is important for the interpretation of experimental MCD data. As for all other magnetic properties, however, the calculation of the MCD parameters is hampered by their unphysical dependence on the origin of the vector potential, encountered when a fixed finite basis set is used. Gauge-origin independence of many magnetic properties may be obtained using the perturbation-dependent

London atomic orbitals,[4,5] often referred to as gauge-including atomic orbitals (GIAOs). Calculations using GIAOs have been successfully carried out for many magnetic properties at various levels of theory including Hartree−Fock (HF),[6−10] second-order Møller−Plesset perturbation theory (MP2),[11−14] and coupled cluster theory−in particular the coupled cluster singles and doubles (CCSD)[15,16] model and the CCSD model with perturbative correction for triples (CCSD(T)).[17] Recently, first and second analytic derivatives have been presented for general coupled cluster schemes[18,19] within the framework of a string-based many-body formalism. Of specific relevance to our study is the implementation of magneto-optical properties (Verdet constants and $\mathscr{B}$ terms) using GIAOs at the CCSD level.[20] GIAOs have also been employed to obtain gauge-origin-independent magnetic properties within density functional theory (DFT),[21] and recently, time-dependent DFT (TD-DFT) has been used in connection with GIAOs for the determination of the Verdet constant.[22] (TD-)DFT is particularly useful, as large molecules may be addressed.[23,24] However, the functionals available at present give a significantly lower accuracy than that obtained in more elaborate wave function calculations. To understand the quality of the results that may be obtained using the different DFT functionals, (TD-)DFT results have therefore

---

MCD of Azabenzenes and Phosphabenzene

J. Phys. Chem. A, Vol. 111, No. 44, 2007 **11279**
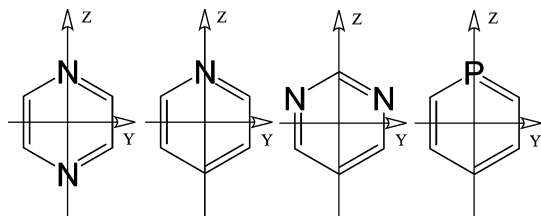
Figure 1. The molecules under investigation, with specification of the coordinate axes. From the left: pyrazine, pyridine, pyrimidine, and phosphabenzene.

often been benchmarked against results from higher-level coupled cluster models.[25-27]

MCD calculations were initially carried out using the sum-over-states (SOS) method.[28-35] The SOS method is time-consuming, as it requires explicit evaluation of the intermediate excited states. In the SOS method, it is often difficult to include a sufficient number of excited states to obtain a converged result. On the other hand, when one or only very few contributions dominate a $\mathscr{B}$ term, the SOS method provides useful intuitive insight into its origin in terms of magnetic-field-induced state mixing, which provides a qualitative predictive capability for related molecules.

Alternatively, the evaluation of the $\mathscr{B}$ term can be based on computation of the first residue of frequency-dependent quadratic response functions involving electric dipole and magnetic dipole operators. Results obtained using such an approach have been presented at the Hartree−Fock and multiconfigurational self-consistent-field levels of theory,[36] and very recently also within TD-DFT.[37] Explicit summation over intermediate excited states is avoided in this approach, as only sets of linear response equations are solved. No treatment of the gauge-origin problem was performed in refs 36 and 37. The $\mathscr{B}$ term has also been computed at the Pariser−Parr−Pople (PPP) level using GIAOs and a finite difference approach where the transition strength is evaluated in the presence of the magnetic field.[38] Coriani et al.[20,39] implemented the analytic analog of this finite difference approach for the CCSD model, starting from the analytical expression for the dipole transition strength obtained from response theory. They carried out test calculations on formaldehyde to demonstrate the gauge-origin independence.[20,39,40] The present study applies the approach of Coriani et al.[20,39] to investigate the $\mathscr{B}$ terms of azabenzenes and phosphabenzene.

The CCSD method is a robust model which gives rather accurate and reliable results for molecular properties of systems that are single-configuration dominated. For this reason, it is interesting to examine the performance of the CCSD-GIAO approach for predicting the $\mathscr{B}$ terms. We presently report calculations on the selected conjugated ring systems given in Figure 1. The calculations reveal interesting information about the experimental spectra, in particular for close lying excited states, where the cancellation of positive and negative $\mathscr{B}$ term contributions is shown to strongly affect both the intensity and position of the experimental peaks.

In the next section, we summarize the theory behind our implementation. In the following section, the computational details are given, and in the fourth section, the calculated results are printed and compared with experiment. The fifth section provides a comparison with previous assignments and interpretations, and the last section contains some concluding remarks.

II. Theory

For a medium which is isotropic in the absence of magnetic fields, the Faraday $\mathscr{B}$ term for the transition from the electronic

(ground) state $|n\rangle$ to the electronic state $|j\rangle$ is defined as (atomic units)[3,41]

$$\mathscr{B}(n \rightarrow j) = \epsilon_{\alpha\beta\gamma}\mathscr{J}\left\{\langle n|\mu_\beta|j\rangle\left(\sum_{k\neq n}\frac{\langle j|\mu_\gamma|k\rangle\langle k|m_\alpha|n\rangle}{\omega_k} + \sum_{k\neq j}\frac{\langle j|m_\alpha|k\rangle\langle k|\mu_\gamma|n\rangle}{\omega_k - \omega_j}\right)\right\} \quad (1)$$

$$\equiv \epsilon_{\alpha\beta\gamma}\mathscr{J}\,[M^{\mu_\beta}_{n\leftarrow j}M^{\mu_\gamma,m_\alpha}_{j\leftarrow n}(0)] \quad (2)$$

m_α indicates the α Cartesian component of the magnetic dipole operator, and μ_α, the corresponding component for the electric dipole operator; $\epsilon_{\alpha\beta\gamma}$ is the alternating Levi−Civita tensor. ($\epsilon_{\alpha\beta\gamma} = 1$ for an even permutation of xyz, and $\epsilon_{\alpha\beta\gamma} = -1$ for an odd one. If any two Cartesian components are equal, for instance, $\alpha = \beta$, the corresponding tensor element is zero.)[42] Implicit summation over repeated Greek indices is assumed. The symbol $\mathscr{J}$ denotes the imaginary part of the quantity in parenthesis. $M^{\mu_\beta}_{n\leftarrow j}$ and $M^{\mu_\gamma,m_\alpha}_{j\leftarrow n}(0)$ are one- and two-photon transition moments, respectively, which are implicitly defined through eq 1. The states involved in the above expression are those for the unperturbed system. The $\mathscr{B}$ term may alternatively be obtained as the total derivative with respect to the magnetic field of the one-photon transition strength $\tilde{S}^{\alpha\beta}_{nj}$:[20,39]

$$\mathscr{B}(n \rightarrow j) = \frac{1}{2}\epsilon_{\alpha\beta\gamma}\mathscr{J}\left(\frac{d\tilde{S}^{\alpha\beta}_{nj}}{dB_\gamma}\right)_{B=0} \quad (3)$$

where

$$\tilde{S}^{\alpha\beta}_{nj} = \langle\tilde{n}|\tilde{\mu}_\alpha|\tilde{j}\rangle\langle\tilde{j}|\tilde{\mu}_\beta|\tilde{n}\rangle = \tilde{M}^{\mu_\alpha}_{n\leftarrow j}\tilde{M}^{\mu_\beta}_{j\leftarrow n} \quad (4)$$

is evaluated in the presence of the magnetic field (the tilde indicates such magnetic-field dependence).[20,38]

Equations 1 and 3 are equivalent for exact states. However, for implementation of the $\mathscr{B}$ term calculation within approximate wave function models and using GIAOs, it is advantageous to employ eq 3, since one can rather easily parametrize the magnetic-field dependence in the transition strength matrix due to both the external magnetic field and the GIAO phase factor, and obtain the $\mathscr{B}$ term by straightforward differentiation with respect to the magnetic-field strength.

In coupled cluster theory, bra and ket states differ and the one-photon transition strength has to be evaluated using a symmetrized expression

$$S^{\alpha\beta}_{nj} = \frac{1}{2}(M^{\mu_\alpha}_{n\leftarrow j}M^{\mu_\beta}_{j\leftarrow n} + (M^{\mu_\beta}_{n\leftarrow j}M^{\mu_\alpha}_{j\leftarrow n})^*) \quad (5)$$

where the explicit expressions for the one-photon transition moments at the CCSD level are given in ref 20. Coriani et al. obtained the $\mathscr{B}$ term from an analytic differentiation of eq 5 with respect to the magnetic field, considering the magnetic-field dependence both on the external magnetic field and on the GIAOs. The GIAOs ensure that the $\mathscr{B}$ term is gauge-origin independent. The working expressions for the derivatives of the left and right one-photon dipole transition moments $M^{\mu}_{n\leftarrow j}$ and $M^{\mu}_{j\leftarrow n}$ are given in eqs 82 and 83 of ref 20, respectively. See also ref 39 for details of the implementation.

III. Computational Details

The CCSD results for the Faraday $\mathscr{B}$ term of MCD have been obtained using a local version of the dalton program[43]

TABLE 1: Pyrazine. CCSD Results for the Second Moments of Charges (au), Vertical Excitation Energies (eV), Oscillator Strengths, and Faraday $\mathscr{B}$ Terms (10^{-3} $D^2\mu_B$cm) for the First Five Transitions from the Ground State

excited state	character	basis set	second moment[a]	excitation energies	oscillator strength	B term
B_{3u}	$n\pi^*$	aug-cc-pVDZ	413	4.33	0.007	−0.061
B_{3u}	$n\pi^*$	aug-cc-pVDZ-CM	413	4.32	0.007	−0.061
B_{3u}	$n\pi^*$	aug-cc-pVTZ	412	4.30	0.006	−0.060
B_{3u}	$n\pi^*$	aug-cc-pVTZ-CM	412	4.30	0.006	−0.060
B_{2u}	$\pi\pi^*$	aug-cc-pVDZ	416	5.17	0.082	0.36
B_{2u}	$\pi\pi^*$	aug-cc-pVDZ-CM	416	5.17	0.082	0.36
B_{2u}	$\pi\pi^*$	aug-cc-pTZ	414	5.14	0.083	0.37
B_{2u}	$\pi\pi^*$	aug-cc-pVTZ-CM	414	5.14	0.083	0.37
B_{1u}	$\pi\pi^*$	aug-cc-pVDZ	419	6.98	0.062	−0.57
B_{1u}	$\pi\pi^*$	aug-cc-pVDZ-CM	420	6.98	0.056	−0.50
B_{1u}	$\pi\pi^*$	aug-cc-pVTZ	416	6.93	0.065	−0.75
B_{1u}	$\pi\pi^*$	aug-cc-pVTZ-CM	417	6.92	0.065	
B_{2u}	$n\sigma^*$	aug-cc-pVDZ	470	7.24	0.042	−1.70
B_{2u}	$n\sigma^*$	aug-cc-pVDZ-CM	483	7.19	0.038	−2.14
B_{2u}	$n\sigma^*$	aug-cc-pVTZ	472	7.42	0.040	−1.95
B_{2u}	$n\sigma^*$	aug-cc-pVTZ-CM	481	7.40	0.037	
B_{1u}	$n\sigma^*$	aug-cc-pVDZ	465	7.44	0.109	1.48
B_{1u}	$n\sigma^*$	aug-cc-pVDZ-CM	482	7.34	0.101	2.65
B_{1u}	$n\sigma^*$	aug-cc-pVTZ	467	7.58	0.124	2.24
B_{1u}	$n\sigma^*$	aug-cc-pVTZ-CM	479	7.53	0.112	

[a] The second moment of the ground state is 413 au (CCSD/aug-cc-pVTZ).

where the $\mathscr{B}$ term is implemented as described by Coriani et al.[20] The geometry of the individual molecules has been optimized using the DFT/B3LYP method in a 6-31G(d,p) basis set. For pyrazine, a basis set investigation was performed using the single-augmented correlation-consistent basis sets aug-pVXZ of Dunning and co-workers[44,45] for X=D and X=T. In addition, basis sets were constructed by adding center-of-mass functions. The center-of-mass functions used are the Rydberg functions, as suggested by Kaufmann et al.,[46] with the quantum number n selected as 3 and $^7/_2$ and where all functions with quantum numbers l up to and including $l_{max} = 2$ are taken for a given quantum number n. The resulting basis sets are indicated in the tables as aug-cc-pVDZ-CM and aug-cc-pVTZ-CM.

In order to compare our estimates of the $\mathscr{B}$ terms with experimentally derived data, it is appropriate to note that the $\mathscr{B}$ term is in general small and difficult to measure.[47] The "experimental" $\mathscr{B}$ term is obtained by integration of the experimental MCD spectrum over the band corresponding to the electronic transition, according to the so-called "method of moments".[48,49] The resulting $\mathscr{B}$ term is given in units of $D^2\mu_B$cm (1 au of $\mathscr{B}$ $[a_0^4 e^3\hbar^{-1}]$ is $\approx$5.88764 × 10^{-5} $D^2\mu_B$cm). The integrated $\mathscr{B}$ term corresponds to the result calculated within the Born−Oppenheimer and Franck−Condon approximations. The validity of the method of moments is limited by the degree of overlap between adjacent bands corresponding to different electronic transitions and by the strength of the vibronic coupling. The complexity of most spectra, due to vibronic coupling and strong overlap, often results in a crude estimate of the magnitude of the $\mathscr{B}$ terms, and the experimentally derived values are then only expected to be slightly better than order-of-magnitude estimates.[50] Furthermore, the theoretical results do not take solvent effects into account; thus, a quantitative agreement with experiment cannot be expected. However, as we shall see, the calculated MCD results turn out to be very useful for the interpretation of the experimental data. The experimental excitation energies that we compare with our calculated vertical excitation energies are taken as the wavenumbers at which the maximum intensity for a given band occurs. These maximum-intensity wavenumbers represent, according to the Franck−Condon approximation, an approximation to the vertical excitation energies. However, these excitation

energies are further subject to uncertainties resulting from zero-point vibrations, the extent of the wave function, and the anharmonic potential.

IV. Results and Discussion

A. Pyrazine. The CCSD results for the vertical excitation energies, oscillator strengths, second moments of charges, and the $\mathscr{B}$ terms of pyrazine for different basis sets are collected in Table 1. We have performed a basis set investigation using the aug-cc-pVDZ, aug-cc-pVDZ-CM, aug-cc-pVTZ, and aug-cc-pVTZ-CM basis sets. The first two excited states, B_{3u} and B_{2u}, are valence states with dominant $n\pi^*$ and $\pi\pi^*$ character, respectively, and their extent, measured by the second moment, is similar to that of the ground state (413 au, CCSD/aug-cc-pVTZ). The basis set effects on the excitation energies, second moments, oscillator strengths, and $\mathscr{B}$ terms are rather small. Already with the aug-cc-pVDZ basis set, these valence excitation results appear to have converged.

The influence of higher correlation effects may be estimated from the CC3 excitation energies in the aug-cc-pVDZ basis set given in Table 2. In this table, we also report the experimental results from Castellan and Michl[50] and from Kaito et al.[51] No significant overlap occurs between the different transitions in the UV or MCD spectra. The effect of triple excitations lowers the CCSD excitation energies by 0.1−0.2 eV. The CCSD vertical excitation energies are found to be 0.3−0.4 eV higher than the experimental excitation energies corresponding to the band center maxima. The effect of triples thus accounts for about half this difference. The residual part of the deviation may be due to the uncertainty that is introduced by identifying experimental vertical excitation energies with band center maxima and to solvent effects. The two sets of experimental values were obtained using two similar solvents, cyclohexane and *n*-heptane, and they differ by as much as 0.1 eV, reflecting not only solvent effects but also uncertainties in the location of absorption and MCD peak maxima of broad bands.

Uncertainties of about 10% are typical for molecular properties obtained at the CCSD level of theory. The CCSD/aug-cc-pVDZ oscillator strengths and $\mathscr{B}$ terms are therefore expected to bear such an uncertainty. In Table 3 are listed the calculated

MCD of Azabenzenes and Phosphabenzene

J. Phys. Chem. A, Vol. 111, No. 44, 2007 **11281**

TABLE 2: Excitation Energies (eV) for the Lowest Transitions of Each Molecule

molecule	state	vertical		experimental	
		CCSD[a]	CC3[a]		
pyrazine	B_{3u}	4.33	4.16	3.97[b]	3.98[e]
	B_{2u}	5.17	5.05	4.77[b]	4.87[e]
	B_{1u}	6.98	6.89		
pyrimidine	B_1	4.64	4.46	4.22[b]	4.29[e]
	B_2	5.51	5.40	5.21[b]	5.17[e]
pyridine	B_1	5.18	4.99	4.41[c]	4.31[e]
	B_2	5.28	5.17	4.96[b]	4.96[e]
phosphabenzene	B_2	4.55	4.43	4.22[d]	
	B_1	5.16	5.00	4.71[d]	
	A_1	5.46	5.39	5.21[d]	

[a] Basis set aug-cc-pVDZ. [b] Experimental results from Castellan and Michl[50] recorded at room temperature in cyclohexane. [c] Experimental excitation energy for the 0−0 vibrational transition of the MCD spectrum from Castellan and Michl[50] recorded in cyclohexane. [d] Experimental results from Waluk et al.[53] recorded at 293 K in cyclohexane. [e] Experimental results from Kaito et al.[53] recorded in *n*-heptane.

oscillator strengths and $\mathscr{B}$ terms together with experimental results.[50,51] Good agreement between the experimental and calculated values is found considering the uncertainties in the experimental data. The third transition, $A_g \rightarrow B_{1u}$, is a valence dominated $\pi\pi^*$ excitation with a slight Rydberg character. The excited-state second moment is a little larger than that of the ground state. No significant change is observed in the calculated excitation energy when CM functions are added, but going from X=D to X=T in the basis set yields some change in the oscillator strength and particularly the $\mathscr{B}$ term. The aug-cc-pVDZ results for this state thus cannot be considered fully converged with respect to basis set. The higher excited states are Rydberg states with a second moment by far larger than the one for the ground state. Going from a DZ to a TZ basis set leads to an increase in the excitation energy of the Rydberg states by about 0.2 eV. This is expected since the Rydberg state has one fewer electron pair to correlate than the ground state: the better description of this electron pair in the TZ basis than in the DZ basis leads to this increase in the excitation energy. The larger extent of the Rydberg states calls for more diffuse functions to obtain properly converged results.

B. Pyrimidine. The calculated results for pyrimidine are collected in Table 4, and in Tables 2 and 3, the calculated values are compared with experiment.[50,51] The second moments for the first three excited states ($n\pi^*$, $\pi\pi^*$, and $n\pi^*$ character) are close to the ground-state second moment, and these states are therefore all valence states. The CCSD vertical excitation energies are about 0.3−0.4 eV larger than the experimental excitation energies associated with band maxima.[50,51] As in pyrazine, the effect of triples accounts for about half of this deviation, as seen from the CC3 vertical excitation energies in Table 2. The CC3 results are calculated using the aug-cc-pVDZ basis set. The aug-cc-pVDZ-CM basis set is not required, since all measured transitions are transitions to valence states, which are well described in an aug-cc-pVDZ basis. The calculated $\mathscr{B}$ terms are in good agreement with those derived from the experimental MCD bands (see Table 3). This is expected, as the experimental peaks are fairly well separated.[50,51]

C. Pyridine. The pyridine results are given in Table 5 and are compared to experimental values in Tables 2 and 3. The first two transitions are two valence excited states and have second moments close to that of the ground state. The second experimental excitation energy is 0.3 eV lower than the calculated vertical CCSD excitation energy, in accordance with previous findings for valence states (see Table 2). The experi-

mental excitation energy for the first transition is almost 0.8− 0.9 eV lower than the calculated first excitation energy. The experimental excitation energy for this transition is not obtained from the UV spectrum, since this spectrum does not contain a peak that can be clearly associated with the first transition. Instead, the transition energy is taken from the vibrationally resolved MCD spectrum and is a 0−0 excitation energy, accounting for the large difference to the calculated vertical excitation energy. The $\mathscr{B}$ terms that are calculated for the two lowest transitions, and in particular the first one, are numerically much larger than the experimental observed values given by Castellan and Michl[50] (Table 3). The poor agreement between calculations and experiment for the two lowest valence excitations is due to the fact that the first $A_1 \rightarrow B_1$ transition (of $n\pi^*$ character) is severely overlapped by the second, much stronger, $A_1 \rightarrow B_2$ transition (of $\pi\pi^*$ character). Since two oppositely signed $\mathscr{B}$ terms are present, they partially cancel in the experimental spectrum. Ideally, a deconvolution of the experimental spectrum would give the $\mathscr{B}$ terms of each transition, but because of the cancellation of positive and negative contributions, no unique solution can be found.

To illustrate the cancellation that occurs between positive and negative contributions to the MCD spectrum, a convolution of the calculated MCD spectrum can be performed. The convolution is done by representing the calculated transition by means of a Gaussian line shape function

$$f(\nu) = \frac{\mathscr{Y}}{\sigma\sqrt{2\pi}} \exp\left[-\frac{(\nu - X)^2}{2\sigma^2}\right] \quad (6)$$

The function f is a function of the wavenumber ν and is centered at the wavenumber X with a line width parameter σ. Note that the traditional expression for a Gaussian line shape function has been modified by introducing the scaling constant $\mathscr{Y}$, calculated as

$$\mathscr{Y} = \mathscr{B}\cdot 33.53 \left(\int \frac{1}{\sigma\sqrt{2\pi}} \exp\left[-\frac{(\nu - X)^2}{2\sigma^2}\right]\nu^{-1}\,d\nu\right)^{-1} \quad (7)$$

such that the integral over the function $f(\nu)$ gives the computed $\mathscr{B}$ term according to the method-of-moments formula[52]

$$\mathscr{B} = -\frac{1}{33.53}\int f(\nu)\nu^{-1}\,d\nu \quad (8)$$

In Figure 2, we have thus simulated the MCD spectrum for the two transitions by representing the calculated transitions by means of two Gaussian line shape functions placed at the CCSD excitation energies ($X = 5.18$ eV and $X = 5.28$ eV) with a line width parameter σ of 1555 cm^{-1}. The line width parameter of 1555 cm^{-1} was taken as the average line width parameter from Gaussian fits of the two lowest well separated peaks of the UV and MCD spectra of pyrimidine (see previous section). Adding together the two Gaussians gives the simulated spectrum (solid line) in Figure 2. Using the method of moments, eq 8, on the simulated spectrum yields the new simulated $\mathscr{B}$ values in Table 6, along with new excitation energies as obtained from the band maxima. The simulated spectrum is in close agreement with the observed spectrum. The first transition is almost completely canceled, and the location of the band center has shifted by 0.44 eV. The maximum of the second transition has hardly moved. When sizable cancellation of positive and negative contributions occurs, the location of the peak maximum may move, introducing uncertainties if one assigns the peak maxima to vertical excitation energies.

TABLE 3: Oscillator Strengths f and Faraday $\mathscr{B}$ Terms (10^{-3} D$^2\mu_B$cm) for the Lowest Transitions of Each Molecule

		vertical		experimental			
molecule	state	f^a	B term^a	f	f	B term	B term
pyrazine	B$_{3u}$	0.007	−0.061	0.01^b	0.0092^d	−0.04^b	−0.047^d
	B$_{2u}$	0.082	0.36	0.08^b	0.081^d	0.4^b	0.46^d
pyrimidine	B$_1$	0.006	−0.068	0.007^b	0.0073^d	−0.06^b	−0.076^d
	B$_2$	0.028	0.210	0.03^b	0.033^d	0.2^b	0.24^d
pyridine	B$_1$	0.005	−0.054			−0.0002^b	
	B$_2$	0.028	0.163	0.04^b	0.041^d	0.1^b	0.15^d
phosphabenzene	B$_2$	0.001	0.157			0.11^c	
	B$_1$	0.019	−0.438			−0.10^c	
	A$_1$	0.163	0.735	0.16^c		0.56^c	

^{a} CCSD response calculations using a aug-cc-pVDZ-CM basis set. ^{b} Experimental results from Castellan and Michl[50] recorded at room temperature in cyclohexane. ^{c} Experimental results from Waluk et al.[53] recorded at 293 K in cyclohexane. ^{d} Experimental results from Kaito et al.[51] recorded in *n*-heptane.

TABLE 4: Pyrimidine. CCSD Results for the Second Moments of Charges (au), Vertical Excitation Energies (eV), Oscillator Strengths, and Faraday $\mathscr{B}$ Terms (10^{-3} D$^2\mu_B$cm) for the First Five Excited States

excited state	character	basis set	second moment^a	excitation energies	oscillator strength	B term
B$_1$	nπ*	aug-cc-pVDZ-CM	413	4.64	0.006	−0.068
B$_2$	$\pi\pi$*	aug-cc-pVDZ-CM	415	5.51	0.028	0.210
B$_1$	nπ*	aug-cc-pVDZ-CM	413	6.51	0.006	−0.055
B$_2$	nσ*	aug-cc-pVDZ-CM	457	6.68	0.008	0.017
A$_1$	$\pi\pi$*	aug-cc-pVDZ-CM	420	6.98	0.027	−0.267

^{a} The second moment of the ground state is 413 au (CCSD/aug-cc-pVDZ-CM).

TABLE 5: Pyridine. CCSD Results for the Second Moments of Charges (au), Vertical Excitation Energies (eV), Oscillator Strengths, and Faraday $\mathscr{B}$ Terms (10^{-3} D$^2\mu_B$cm) for the First Six Transitions from the Ground State

excited state	character	basis set	second moment^a	excitation energies	oscillator strength	B term
B$_1$	nπ*	aug-cc-pVDZ-CM	437	5.18	0.005	−0.054
B$_2$	$\pi\pi$*	aug-cc-pVDZ-CM	439	5.28	0.028	0.163
A$_1$	$\pi\pi$*	aug-cc-pVDZ-CM	461	6.71	0.003	−0.042
A$_1$	nσ*	aug-cc-pVDZ-CM	466	6.79	0.027	−0.365
B$_1$	$\pi\sigma$*	aug-cc-pVDZ-CM	503	7.27	0.041	−1.547
B$_2$	nσ*	aug-cc-pVDZ-CM	511	7.34	0.008	−2.300

^{a} The second moment of the ground state is 437 au (CCSD/aug-cc-pVDZ-CM).
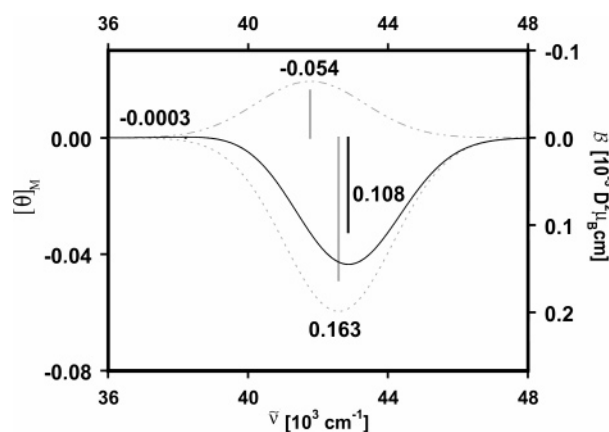
Figure 2. Pyridine. The gray sticks give the calculated $\mathscr{B}$ terms, while the gray dashed lines give the corresponding Gaussian line shape functions. Superimposing the Gaussians gives the simulated theoretical spectrum (black solid line) with the black sticks representing the $\mathscr{B}$ terms obtained from integration of the simulated theoretical spectrum. The numbers in the figure refer to the size of the $\mathscr{B}$ terms. The black stick of size -0.0003×10^{-3} D$^2\mu_B$cm at 38231 cm^{-1} is not visible on the scale used.

In the theoretical simulated spectrum (Table 6), the $\mathscr{B}$ term for the intense second transition is in good agreement with the experimental value while a relatively large deviation is seen for the first weak transition. However, considering the large cancellation of positive and negative contributions for this transition and its weakness, the discrepancy appears to be acceptable.

TABLE 6: Pyridine. Comparison of Results for the Excitation Energies and $\mathscr{B}$ Terms Obtained from Direct Calculation, Theoretically Simulated Spectra, and Experiment (Excitation Energies Are Given in eV; $\mathscr{B}$ Terms Are Given in Units of 10^{-3} D$^2\mu_B$cm)

			calculated values			
	experimental^a		vertical		simulated	
excited state	excitation energies	B term	excitation energies	B term	excitation energies	B term
B$_1$	4.41	−0.0002	5.18	−0.054	4.74	−0.0003
B$_2$	4.96	0.1	5.28	0.163	5.31	0.108

^{a} Experimental results from Castellan and Michl.[50]

In Figure 3, the theoretical spectrum (dashed line) has been parallel displaced by 2200 cm^{-1} (0.27 eV) and superimposed onto the experimental spectrum[50] (the solid line). Good agreement between the theoretical and experimental spectra is now observed. CC3 calculated excitation energies (Table 2) show that about 0.15 eV of the parallel displacement has its origin in correlation effects beyond CCSD. We attribute the rest of the displacement to the uncertainty associated with assigning experimental band centers to vertical excitation energies and to solvent effects.

The experimental oscillator strength for the second transition is slightly larger than the calculated value. Experimentally, no strength has been assigned to the lowest transition, and its strength was thus added to the value of the second transition. The CCSD calculations indicate that the first transition is located about 0.1 eV below the second transition. Assigning a line width of 1555 cm^{-1} to the lowest two transitions gives the simulated

MCD of Azabenzenes and Phosphabenzene

J. Phys. Chem. A, Vol. 111, No. 44, 2007 **11283**
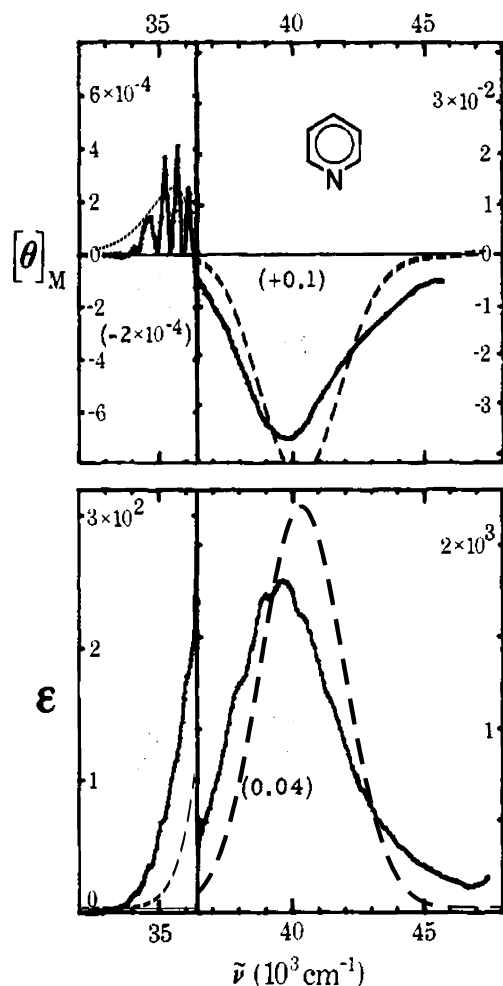
Figure 3. Pyridine. The solid line is the experimental spectrum observed by Castellan and Michl,[50] and the dashed line is the simulated spectrum: top, MCD (experimental $\mathscr{B}$ terms given in 10^{-3} $D^2\mu_B$cm); bottom, absorption (experimental oscillator strengths given).

spectrum (dashed line), which in Figure 3 is parallel displaced by the same amount (2200 cm^{-1}), as was done for the MCD spectrum in the upper panel of Figure 3. The first transition is completely merged with the second transition in the simulated UV spectrum (see Figure 3). The experimental MCD spectrum was used to obtain the first transition energy. Due to strong overlap, the peak maximum was shifted to a much lower value. Experimentally, the lowest excitation energy is assigned to a 0−0 vibrational transition energy and thus not a vertical excitation energy.

D. Phosphabenzene. The results calculated for phosphabenzene are collected in Table 7. The calculated second moments reveal that all of the examined excited states, except the B_1 state at 6.18 eV and the A_1 state at 6.78 eV, have valence character. Therefore, all of the low-energy transitions may be expected to be well described in the aug-cc-pVDZ basis. The CCSD vertical excitation energies are all found to be 0.3−0.4 eV above the experimental values of Waluk et al.[53] (see Table 2), in accordance with the observations for the other low-lying valence excitations of this investigation.

The absorption spectrum of phosphabenzene is completely dominated by the third transition measured at 5.21 eV. Its calculated oscillator strength is 0.16, in good agreement with the observed value.[53] The oscillator strength is 1 order of magnitude smaller for the second transition (measured at 4.71 eV), which is of $n\pi^*$ character, and another order of magnitude smaller for the first transition measured at 4.22 eV,

which is of the $\pi\pi^*$ type. Assigning a line width parameter of 1555 cm^{-1} to the lowest six transitions gives the simulated spectrum (dashed line), which in Figure 5 is parallel displaced by 3000 cm^{-1} (0.37 eV). The simulated spectrum is in good agreement with the experimental absorption spectrum where the first two transitions only appear as shoulders on the band for the strong transition. However, the presence of the two transitions is revealed clearly in the MCD spectrum. Contrary to what is observed for the oscillator strength, the calculated $\mathscr{B}$ terms for the three lowest transitions are all of the same order of magnitude. However, large deviations are found between the calculated and experimental $\mathscr{B}$ terms (Table 3). As for pyridine, these deviations can be attributed to oppositely signed overlapping bands and a corresponding partial cancellation of the $\mathscr{B}$ terms.

In Figure 4, we have carried out a theoretical simulation of the MCD spectrum by placing Gaussian line shape functions at the theoretically calculated excitation energies. The individual Gaussian functions were assigned a line width parameter of σ = 1555 cm^{-1} for all excitations, similar to what was done for pyridine. A subsequent summation of the Gaussians gives the solid line and the simulated theoretical spectrum in Table 8. The location of the band centers is hardly changed in the simulated spectrum, but the cancellation does have a significant impact, as the fourth transition with a calculated excitation energy of 6.18 eV vanishes completely. The theoretical simulated $\mathscr{B}$ terms correspond quite well to the experimental ones, though the numerical values are still a little too high. A small adjustment in the line width leads to very close agreement between the experimental and simulated spectra.

In Figure 5, we have superimposed the simulated theoretical spectrum onto the experimental one[53] with a parallel displacement of 3000 cm^{-1} (0.37 eV). A good agreement is seen between the experimental and simulated spectra. The experimental results from Waluk et al.[53] suggest a positive fourth $\mathscr{B}$ term. Although no quantitative results were achieved, this is also in agreement with our simulated spectrum. The CC3 calculated excitation energies in Table 2 indicate that about half of the parallel displacement has its origin in correlation effects beyond CCSD. The residual part of the deviation may be attributed to uncertainties related to assigning experimental band centers to vertical excitation energies and solvent effects.

V. Comparison with Earlier Assignments and Interpretations

The primary value of simple traditional models is their ability to provide intuitive understanding and facile predictions of trends for series of related compounds. The traditional analysis of the low-energy electronic states of perturbed benzenes and their absorption and MCD spectra is based on the perimeter model and the SOS approach, which are simple enough to allow algebraic solutions.[54−57] In its simplest form, the perimeter model considers the four states that result from single excitations from the doubly degenerate highest occupied molecular orbital (HOMO) of benzene into its doubly degenerate lowest unoccupied MO (LUMO). When the MOs are chosen in their complex form, electron circulation sense-conserving excitations are at higher energy and give rise to the degenerate and dipole allowed B state, whereas the sense-reversing excitations interact and their combinations result in the lower-energy dipole-forbidden L_b and L_a states. The perimeter model says nothing about the $\mathscr{B}$ terms and absorption intensities of $n\pi^*$ states, and their quite accurate description obtained here represents a great strength and advantage of the ab initio approach.

TABLE 7: Phosphabenzene. CCSD Results for the Second Moments of Charges (au), Vertical Excitation Energies (eV), Oscillator Strengths, and Faraday $\mathscr{B}$ Terms (10^{-3} D$^2\mu_B$cm) for the First Six Transitions from the Ground State

excited state	character	basis set	second moment[a]	excitation energies	oscillator strength	B term
B$_2$	$\pi\pi^*$	aug-cc-pVDZ-CM	593	4.55	0.001	0.157
B$_1$	nπ^*	aug-cc-pVDZ-CM	591	5.16	0.019	−0.438
A$_1$	$\pi\pi^*$	aug-cc-pVDZ-CM	595	5.46	0.163	0.735
B$_1$	$\pi\sigma^*$	aug-cc-pVDZ-CM	640	6.18	0.005	0.042
B$_2$	$\pi\pi^*$	aug-cc-pVDZ-CM	595	6.36	0.259	2.351
A$_1$	$\pi\pi^*$	aug-cc-pVDZ-CM	619	6.78	0.343	−4.795

[a] The second moment of the ground state is 591 au (CCSD/aug-cc-pVDZ-CM).
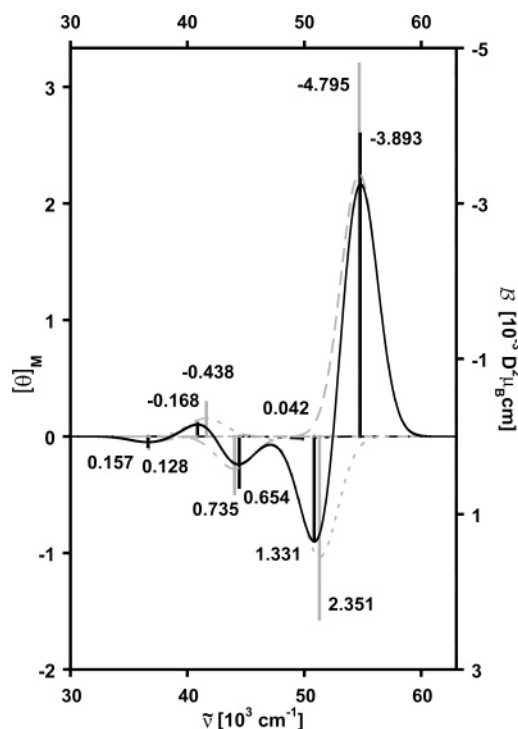
Figure 4. Phosphabenzene. The gray sticks give the calculated $\mathscr{B}$ terms, while the gray dashed lines give the corresponding Gaussian line shape functions. Superimposing the Gaussians give the simulated theoretical spectrum (black solid line) with the black sticks representing the $\mathscr{B}$ terms obtained from integration of the simulated theoretical spectrum. The numbers in the figure refer to the size of the $\mathscr{B}$ terms.

The perimeter model produces the correct trends in intensities and also MCD signs, but one could ask whether this agreement is accidental. In principle, accurate ab initio theory is not only able to reproduce the measured spectra but should also permit the testing of the assumptions and of the unobservable intermediate results of the traditional models, providing a much stricter test than mere comparison of the final results with experiment. Demonstrating the ability of an ab initio method to reproduce the observed oscillator strengths and $\mathscr{B}$ term, as has been done here, represents the first step toward such a test. Obtaining and comparing some of the intermediate results would be the next logical step. For instance, it would be useful to see a justification of the assumption that underlies the application of the perimeter model to MCD spectra, namely, that magnetic mixing with nπ^*, $\sigma\pi^*$, and $\pi\sigma^*$ states has a negligible effect on the $\mathscr{B}$ terms of $\pi\pi^*$ states. At the moment, the only intermediate results that can be compared are MO shapes and relative energies, and the amplitude of one-electron excitations that enter the description of the excited states. These agree well with expectations based on the traditional perimeter model, although the comparison is not always straightforward, due to the presence of a large number of virtual orbitals in the ab initio description.
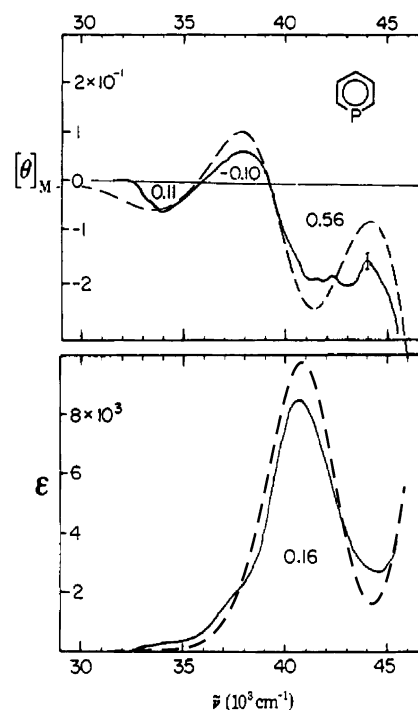
Figure 5. Phosphabenzene. The solid line is the experimental spectrum observed by Waluk et al.,[53] and the dashed line is the simulated spectrum: top, MCD (experimental $\mathscr{B}$ terms given in 10^{-3} D$^2\mu_B$cm); bottom, absorption (experimental oscillator strengths given).

TABLE 8: Phosphabenzene. Comparison of Results for the Excitation Energies and $\mathscr{B}$ Terms Obtained from Direct Calculation, Theoretically Simulated Spectra, and Experiment (Excitation Energies Are Given in eV; $\mathscr{B}$ Terms Are Given in Units of 10^{-3} D$^2\mu_B$cm)

			calculated values			
	experimental values[a]		vertical		simulated	
excited state	excitation energies	B term	excitation energies	B term	excitation energies	B term
B$_2$	4.22	0.11	4.55	0.158	4.54	0.128
B$_1$	4.71	−0.10	5.16	−0.438	5.07	−0.168
A$_1$	5.21	0.56	5.46	0.735	5.50	0.654
B$_1$			6.18	0.042		
B$_2$			6.36	2.351	6.31	1.331
A$_1$			6.78	−4.795	6.85	−3.893

[a] Experimental results from Waluk et al.[53]

Briefly, in the perimeter model,[58−60] the low-energy $\pi\pi^*$ excited states of the four heterocycles can be viewed as perturbed B$_{2u}$ (L$_b$) and B$_{1u}$ (L$_a$) states of benzene. In the parent, they are electronically forbidden and gain intensity by vibronic coupling to the strongly allowed E$_{1u}$ (B) state, which lies above 6 eV and is not observed in the experiments discussed here. In the description of the $\pi\pi^*$ states of the three azines,[50] the perturbation is primarily due to the increased electronegativity of nitrogen relative to carbon. This is taken to be a one-electron perturbation, and its effect on two-electron integrals and on the

MCD of Azabenzenes and Phosphabenzene

J. Phys. Chem. A, Vol. 111, No. 44, 2007 **11285**

MO coefficients is neglected. The only effect of single or multiple aza replacement in benzene that is considered is the splitting of the degeneracy. In pyridine and pyrazine, it induces the **s**, **a**, −**s**, −**a** orbital ordering of the π MOs in the order of increasing energy, where the MO **s** is the symmetric and the MO **a** is the antisymmetric bonding orbital relative to a plane of symmetry that is perpendicular to the molecular plane and passes through atoms, and −**s** and −**a** are their antibonding counterparts. In pyrimidine, it induces the **a**, **s**, −**a**, −**s** ordering. Because of the alternant pairing of bonding and antibonding orbitals, to first order in perturbation theory, the **s**, **a** orbital energy difference (ΔHOMO) is the same as the −**s**, −**a** orbital energy difference (ΔLUMO), and since the effect of the aza replacement on two-electron terms has been neglected, this means that the **s** → −**s** and **a** → −**a** promotions are degenerate. The perturbation is even in the sense of Moffitt[59] and causes the L_b state to obtain intensity from the B state, because the **s** → −**a** and **a** → −**s** promotions are no longer degenerate, as they were in benzene.

According to the perimeter model of MCD spectroscopy of annulenes and their derivatives, this still leaves the L_b state with an only weakly positive $\mathscr{B}$ term due to the so-called μ^- contribution, since the potentially much larger μ^+ contribution vanishes when ΔHOMO and ΔLUMO are equal (μ_- is the difference and μ_+ is the sum of the out-of-plane components of the magnetic dipole moments of an electron in the LUMO and the HOMO). Going beyond first order in perturbation theory, one finds that ΔHOMO is somewhat larger than ΔLUMO. This gives the perturbation some odd character in the sense of Moffitt, allows the L_a state to obtain intensity from the B state as well, and increases the positive $\mathscr{B}$ term of the L_b transition by providing a positive μ^+ contribution. The L_b transition is the only $\pi\pi^*$ transition observed in the spectra, and its calculated nature is that expected from the perimeter model, a mixture of **s** → −**a** and **a** → −**s** excitation amplitudes. In pyridine and pyrazine, where the order of orbital energies is **s**, **a**, −**s**, −**a**, the **a** → −**s** excitation has a larger weight, and in pyrimidine, where the order is **a**, **s**, −**a**, −**s**, the **s** → −**a** excitation is more important.

The situation is more interesting in the case of phosphabenzene.[53] Here, a perimeter model interpretation was based on the assumption that the lowest of the three observed $\mathscr{B}$ terms was due to an $n\pi^*$ transition, followed by two $\pi\pi^*$ transitions, L_b and L_a. This seemed reasonable in view of the relative intensities of the bands, but there was no direct evidence for it. From the observed MCD signs, it was then concluded that ΔHOMO is smaller than ΔLUMO, which implied (i) that the long C−P bond causes a significant weakening of the π interaction relative to the benzene C−C bond, inducing the orbital ordering **a**, **s**, −**s**, −**a**, different from what it is in pyridine, and (ii) that, in the π system, the phosphorus $3p_z$ orbital was effectively more electronegative than the carbon $2p_z$ orbital and acted as an electron acceptor. The present ab initio results agree with the **a**, **s**, −**s**, −**a** orbital ordering deduced from the MCD signs using the perimeter model. However, the very weak first transition is now calculated to be $\pi\pi^*$ and the much stronger second transition is now assigned as $n\pi^*$, reversing the previously assumed state assignment. If this reassignment is correct, the $\mathscr{B}$ terms of both the L_b and the L_a transitions are therefore negative. The newly proposed assignment is verifiable by polarization spectroscopy, but the measurement has not yet been done.

According to the perimeter model, the negative sign for both L transitions is only compatible with similar values of the orbital energy differences ΔHOMO and ΔLUMO. This is exactly the result obtained in our calculations, according to which the weights of the out-of-phase combined **s** → −**a** and **a** → −**s** excitations in the transition to the L_b state are nearly equal, with amplitudes of 0.6 and −0.6. This result is also immediately apparent from the nearly vanishing intensity of the newly assigned L_b transition, in which the contributions from the two excitations approximately cancel. The computations are thus perfectly compatible with expectations based on the perimeter model once the states are reassigned. They also agree with the perimeter model in ascribing the **s** → −**s** excitation as the dominant amplitude (0.8) in the L_a transition. The excitation that is calculated to dominate the $n\pi^*$ transition is **n** → −**s**.

Once the argument for ΔHOMO < ΔLUMO disappears, so does the surprising conclusion[53] that the π symmetry AO on phosphorus must be more electronegative than that on carbon. Using the arguments of ref 53, similar values of ΔHOMO and ΔLUMO imply similar electronegativities for the π orbitals on C and P. This is an intuitively more satisfactory conclusion than the one based on the original state assignment used in ref 53. The similarity to the spectra of a related compound, arsabenzene,[53] argues that the electronegativity is similar for the As atom. The increase in the positive $\mathscr{B}$ term of the L_b transition and the decrease in the positive term of the L_a transition upon going to stibabenzene, on the other hand, suggest that the effective electronegativity of the π symmetry AO on the Sb atom is lower. The conclusions are equally compatible with the methyl substituent effects reported for arsabenzene,[53] if the state assignments are similar to those in phosphabenzene. Introduction of a methyl into position 4 of arsabenzene would be expected to increase ΔHOMO relative to ΔLUMO somewhat, and therefore to make the $\mathscr{B}$ term of the L_b transition more positive and that of the L_a transition less positive, exactly as observed, while 2-methyl substitution should have little effect, as it does.

VI. Summary and Conclusion

Gauge-origin-independent calculations of the Faraday $\mathscr{B}$ term of MCD have been presented for a series of conjugated molecules using the coupled cluster singles and doubles (CCSD) model and London orbitals. The $\mathscr{B}$ term can have both positive and negative values and is therefore a good supplement to UV spectra, for instance, for identifying molecular excited states hidden under overlapping bands.

For non-overlapping bands, the $\mathscr{B}$ terms calculated at the CCSD level at the equilibrium geometries of all four heterocycles are in good agreement with the experimental values. For overlapping bands, large deviations occur. When a line width is attributed to the calculated values of the $\mathscr{B}$ terms, a large cancellation of positive and negative contributions occurs, improving significantly the agreement between the theoretical and experimental spectra. The cancellation between positive and negative contributions results in some cases in a large displacement of the band center maximum (pyridine), and assigning the maximum to a vertical excitation energy then leads to large errors in the assigned "vertical experimental excitation energies". Bands may also completely vanish (phosphabenzene) due to the cancellation of positive and negative contributions. The cancellation between the positive and negative contributions leads to a significant reduction of the B terms compared to the calculated $\mathscr{B}$ terms and to a good agreement with experiment when the theoretical spectrum is parallel displaced. A major contribution for this displacement is the shift in the excitation energies due to correlation beyond CCSD, as seen when comparing vertical CCSD and CC3 excitation energies.

The calculated CCSD MCD results confirm the assignments based on the qualitative results of the perimeter model for the three azines but suggest a new assignment for phosphabenzene which corrects a previous conclusion by showing that the π symmetry AO of phosphorus has a similar electronegativity to that of carbon.

The high quality of the CCSD $\mathscr{B}$ terms makes these values useful for the direct assignment of experimental spectra. The CCSD results may also be useful as benchmarks for judging the quality of Kohn−Sham DFT results, when benchmarking against experimental results cannot be performed because of the cancellation of positive and negative contributions.

References and Notes

(1) Faraday, M. *Philos. Mag.* **1846**, *28*, 294.
(2) Faraday, M. *Philos. Trans. R. Soc. London* **1846**, *136*, 1.
(3) Buckingham, A. D.; Stephens, P. J. *Annu. Rev. Phys. Chem.* **1966**, *17*, 399.
(4) Helgaker, T.; Jørgensen, P. *J. Chem. Phys.* **1991**, *95*, 2595.
(5) London, F. *J. Phys. Radium* **1937**, *8*, 397.
(6) Wolinski, K.; Hinton, J. F.; Pulay, P. *J. Am. Chem. Soc.* **1990**, *112*, 8251.
(7) Häser, M.; Ahlrichs, R.; Baron, H. P.; Weis, P.; Horn, H. *Theor. Chim. Acta* **1992**, *82*, 455.
(8) Pulay, P. *Adv. Chem. Phys.* **1987**, *69*, 241.
(9) Hameka, H. *Mol. Phys.* **1958**, *1*, 203.
(10) Ditchfield, R. *J. Chem. Phys.* **1972**, *56*, 5688.
(11) Gauss, J. *Chem. Phys. Lett.* **1992**, *191*, 614.
(12) Gauss, J. *J. Chem. Phys.* **1993**, *99*, 3629.
(13) Buhl, M.; Thiel, W.; Fleischer, U.; Kutzelnigg, W. *J. Phys. Chem.* **1995**, *99*, 4000.
(14) Fukui, H.; Miura, K.; Matsuda, H. *Chem. Phys. Lett.* **1992**, *96*, 2039.
(15) Gauss, J.; Stanton, J. *J. Chem. Phys.* **1995**, *103*, 3561.
(16) Gauss, J.; Stanton, J. *J. Chem. Phys.* **1995**, *102*, 251.
(17) Gauss, J.; Stanton, J. F. *J. Chem. Phys.* **1996**, *104*, 2574.
(18) Kállay, M.; Gauss, J.; Szalay, P. *J. Chem. Phys.* **2003**, *119*, 2991.
(19) Kállay, M.; Gauss, J. *J. Chem. Phys.* **2004**, *120*, 6841.
(20) Coriani, S.; Hättig, C.; Jørgensen, P.; Helgaker, T. *J. Chem. Phys.* **2000**, *113*, 3561.
(21) Schreckenbach, G.; Ziegler, T. *J. Phys. Chem.* **1995**, *99*, 606.
(22) Krykunov, M.; Banerjee, A.; Ziegler, T.; Autschbach, J. *J. Chem. Phys.* **2005**, *122*, 074105.
(23) Gross, E. K. U.; Dobson, J. F.; Petersilka, M. In *Density Functional Theory II*; Nalewajski, R., Ed.; Topics of Current Chemistry, Vol. 181; Springer: Berlin, 1996; p 81.
(24) van Leeuwen, R. *Int. J. Mod. Phys. B* **2001**, *15*, 1969.
(25) de Oliveira, G.; Martin, J.; de Proft, F.; Geerlings, P. *Phys. Rev. A* **1999**, *60*, 1034.
(26) Wilson, P.; Amos, R.; Handy, N. *Phys. Rev. A* **2000**, *506*, 335.
(27) Pecul, M.; Helgaker, T. *Int. J. Mol. Sci.* **2003**, *4*, 143.
(28) Miles, D. W.; Eyring, H. *Proc. Natl. Acad. Sci. U.S.A.* **1973**, *70*, 3754.
(29) Meier, A. R.; Wagniere, G. H. *Chem. Phys.* **1987**, *113*, 287.
(30) Shieh, D. J.; Lin, S. H.; Eyring, H. *J. Phys. Chem.* **1972**, *76*, 1844.
(31) Goldstein, E.; Vijaya, S.; Segal, G. A. *J. Am. Chem. Soc.* **1980**, *102*, 6198.
(32) Marconi, G. *Chem. Phys. Lett.* **1988**, *146*, 259.
(33) Warnick, M.; Michl, J. *J. Am. Chem. Soc.* **1974**, *96*, 6280.
(34) Fleischhauer, J.; Michl, J. *J. Phys. Chem. A* **2000**, *104*, 7776.
(35) Honda, Y.; Hada, M.; Ehara, M.; Nakatsujia, H.; Michl, J. *J. Chem. Phys.* **2005**, *123*, 164113.
(36) Coriani, S.; Jørgensen, P.; Rizzo, A.; Ruud, K.; Olsen, J. *Chem. Phys. Lett.* **1999**, *300*, 61.
(37) Solheim, H.; Frediani, L.; Ruud, K.; Coriani, S. *Theor. Chem. Acc.* **2007**.
(38) Seamans, L.; Linderberg, J. *Mol. Phys.* **1972**, *24*, 1393.
(39) Coriani, S. Ab initio determination of molecular properties. Ph.D. Thesis, Aarhus University, Denmark, 2000.
(40) Christiansen, O.; Coriani, S.; Gauss, J.; Hättig, C.; Jørgensen, P.; Pawłowski, F.; Rizzo, A. In *Non-Linear Optical Properties of Matter. From molecules to condensed phases*; Papadopoulos, M., Sadlej, A. J., Leszczynski, J., Eds.; Challenges and Advances in Computational Chemistry and Physics, Vol. 1; Springer: Germany, 2006; pp 51−99.
(41) Barron, L. D. *Molecular Light Scattering and Optical Activity*; Cambridge University Press: Cambridge, U.K., 1982.
(42) Moss, R. E. *Advanced Molecular Quantum Mechanics*; Chapmann and Hall Ltd: London, 1973.
(43) Helgaker, T.; Jensen, H. J. Å.; Jørgensen, P.; Olsen, J.; Ruud, K.; Ågren, H.; Auer, A. A.; Bak, K. L.; Bakken, V.; Christiansen, O.; Coriani, S.; Dahle, P.; Dalskov, E. K.; Enevoldsen, T.; Fernandez, B.; Hättig, C.; Hald, K.; Halkier, A.; Heiberg, H.; Hettema, H.; Jonsson, D.; Kirpekar, S.; Kobayashi, R.; Koch, H.; Mikkelsen, K. V.; Norman, P.; Packer, M. J.; Pedersen, T. B.; Ruden, T. A.; Sanchez, A.; Saue, A.; Sauer, S. P. A.; Schimmelpfennig, B.; Sylvester-Hvid, K. O.; Taylor, P. R.; Vahtras, O. *dalton, An electronic structure program*, release 1.2; 2001. See http://www.kjemi.uio.no/software/dalton/dalton.html.
(44) Dunning, T. H., Jr. *J. Chem. Phys.* **1989**, *90*, 1007.
(45) Kendall, R. A.; Dunning, T. H., Jr.; Harrison, R. J. *J. Chem. Phys.* **1992**, *96*, 6796.
(46) Kaufmann, K.; Baumeister, W.; Jungen, M. *J. Phys. B* **1989**, *22*, 2223.
(47) Snyder, P. A.; Hansen, R. W. C.; Rowe, E. M. *J. Phys. Chem.* **1996**, *100*, 17756.
(48) Henry, C. H.; Schnatterly, S. E.; Slichter, C. P. *Phys. Rev.* **1965**, *137*, A583.
(49) Stephens, P. J. *Chem. Phys. Lett.* **1968**, *2*, 241.
(50) Castellan, A.; Michl, J. *J. Am. Chem. Soc.* **1978**, *100*, 6824.
(51) Kaito, A.; Hatano, M.; Tajiri, A. *J. Am. Chem. Soc.* **1977**, *99*, 5241−5246.
(52) Schatz, P. N.; McCaffery, A. J. *Q. Rev. Chem. Soc.* **1969**, *23*, 552.
(53) Waluk, J.; Klein, H.; Ashe, A. J.; Michl, J. *Organometallics* **1989**, *8*, 2804.
(54) Michl, J. *J. Am. Chem. Soc.* **1978**, *100*, 6801.
(55) Michl, J. *J. Am. Chem. Soc.* **1978**, *100*, 6812.
(56) Castellan, A.; Michl, J. *J. Am. Chem. Soc.* **1978**, *100*, 6819.
(57) Michl, J. *Tetrahedron* **1984**, *40*, 3845.
(58) Platt, J. *J. Chem. Phys.* **1949**, *17*, 484.
(59) Moffitt, W. *J. Chem. Phys.* **1954**, *22*, 320.
(60) Moffitt, W. *J. Chem. Phys.* **1954**, *22*, 1820.